

A. N. Ernst, M. H. Somerville, and J. A. del Alamo

Massachusetts Institute of Technology, Cambridge, MA 02139

Abstract

We have carried out pulsed measurements of the *kink effect* in InAlAs/InGaAs on InP HEMTs with nanosecond resolution. Our measurements show that the kink turns on first the higher V_{DS} is. The rate at which the kink builds-up is seen to increase with both V_{DS} and V_{GS} . In general, the kink's characteristic time constant strongly depends on V_{DS} and V_{GS} . Values between 50 ns and 100 μ s have been measured in a single device. These data should be instrumental in formulating a hypothesis for the physical origin of the kink.

I. Introduction

InAlAs/InGaAs high electron mobility transistors (HEMTs) show significant promise for low-noise and high-power millimeter-wave applications. A significant anomaly in their behavior is the *kink effect*, a sudden rise in drain current at a certain drain-to-source voltage that results in high drain conductance and g_m compression, leading to reduced voltage gain and poor linearity. The physical origin of the kink is an issue of considerable contention at this time. Conventional wisdom has attributed the kink effect to traps or their interaction with high-fields or impact ionization (II) [1]-[3]. Recently, simulations [4] as well as light emission, channel-engineering and body contact experiments [5]-[7] have suggested a link between impact ionization and the kink. Indeed, measurements showing direct correlation between II and the kink have been presented [8]. Several models involving II have been proposed including pure II [9], an SOI-like mechanism [7], hole trap charging [10], and *conductivity modulation* of the source [11]-[12].

A new perspective on this problem can be obtained by studying the dynamics of the kink under pulsed operation. Besides providing insight about the origin of the kink, pulsed characterization has been proven to be a good predictor of large-signal high-frequency performance [13]. In this work we have carried out the first experimental time-domain study of the kink effect in InAlAs/InGaAs on InP HEMTs with nanosecond resolution.

II. Experimental

We have designed a pulsed I-V setup able to measure drain response transients with nanosecond resolution. The setup is illustrated in fig. 1 and works as follows: the drain is biased via a DC power sup-

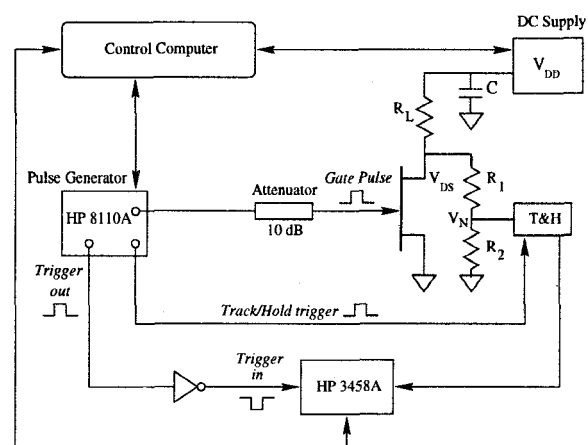


Figure 1: Pulsed I-V setup used in this work.

ply (V_{DD}) and a load resistance, R_L ($R_L = 50 \Omega$). The current drawn by the transistor is evaluated by measuring the voltage at the drain through the R_1/R_2 voltage divider, which is required to protect the T&H due to its limited maximum input voltage. The gate is pulsed from threshold to the desired gate-to-source voltage, V_{GS} , by a dual pulsed generator (PG). The 10 dB attenuator is used to minimize reflections due to impedance mismatch between the 50Ω environment presented by the cables and the gate. After a programmable delay (T_d) from the gate pulse, a second pulse is sent to a track-and-hold amplifier (T&H). When triggered, the T&H holds constant the voltage read at node V_N at the instant of the trigger. This allows a voltmeter to read V_N when triggered by the PG. The relative delays between the pulses sent from the PG to the gate, T&H, and voltmeter are independently programmable and have nanosecond resolution. Once $V_N(T_d)$ is known, $V_{DS}(T_d)$ and $I_D(T_d)$ are easily calculated. The whole schematic is implemented in a specially designed high-speed board to mini-

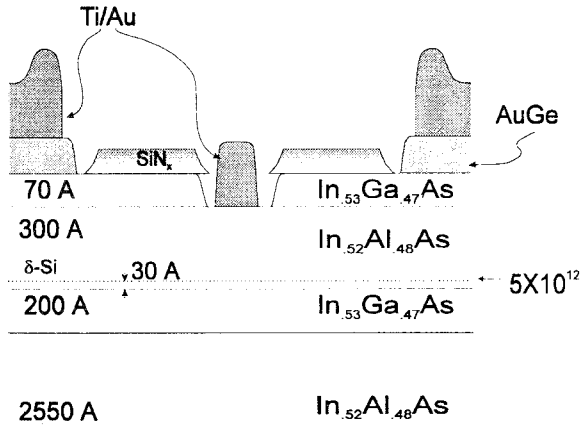


Figure 2: Schematic cross-section of InAlAs/InGaAs single-heterostructure HEMT used in this work.

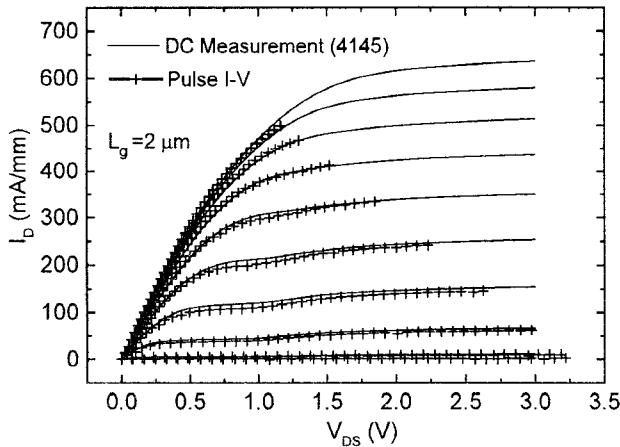


Figure 3: Pulsed I-V set-up validation: pulsed I-V curves for $T_d \approx 500 \mu\text{s}$ (crossed-lines) are compared with DC HP-4145B I-V curves (full lines). Good agreement is observed.

mize wire inductance, crosstalk, and ground bouncing. Measurements are carried out “on-wafer” using coplanar microwave probes. All components have a bandwidth of at least 4 GHz. All measurements have been carried out at room temperature.

In order to trace the whole $I_D - V_{DS}$ plane, for given V_{GS} and T_d , V_{DD} is swept in incremental steps from 0 V to $V_{DD,max}$, where $V_{DD,max}$ is kept below the off-state breakdown voltage. This procedure is then repeated for several values of V_{GS} . For each $V_{DD} - V_{GS}$ pair, T_d samples between 5 ns to 500 μs are acquired.

As a vehicle for this study we used a lattice-matched, MBE-grown, InAlAs/InGaAs HEMT schematically illustrated in fig. 2. The layer structure consists of a 2550 Å InGaAs buffer, a 200 Å InGaAs channel, a 300 Å pseudo-insulator, and a 70 Å InGaAs cap. A delta-doped electron supply layer located 30 Å above the channel yields a sheet carrier

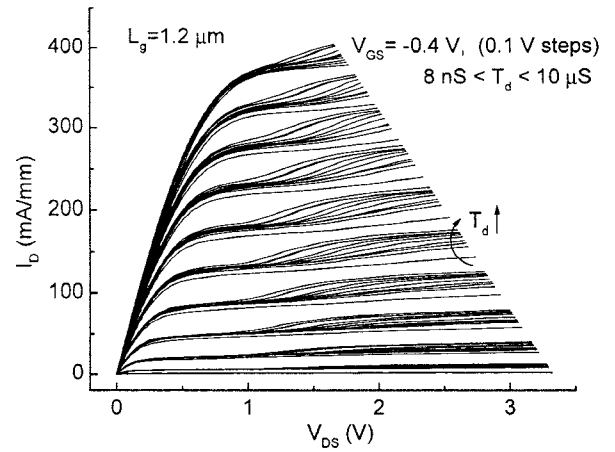


Figure 4: Pulsed I-V curves for varying delay times, T_d . No kink is seen below $T_d = 10 \text{ ns}$. For a given V_{GS} , the larger V_{DS} , the earlier the kink turns on and the faster it saturates.

concentration of $3.6 \times 10^{12} \text{ cm}^{-2}$. Fabrication consists of device isolation via a mesa etch with sidewall recess, a PECVD Si_3N_4 layer for liftoff assistance, Au/Ge ohmic contacts, a selective gate recess, and Pt/Ti/Au gates and interconnects [8, 12]. Devices with gate lengths 1.2 μm and 2 μm were characterized. The devices exhibit $I_{D,max} = 700 \text{ mA/mm}$, $g_{m,peak} = 540 \text{ mS/mm}$, and $BV_{DS(off)} \approx 5 \text{ V}$.

The setup was validated by measuring pulsed I-V characteristics for relatively long T_d ($T_d \approx 500 \mu\text{s}$) and comparing them with DC characteristics obtained using an HP-4145B. Good agreement was observed as shown in fig. 3.

III. Results and Discussion

Pulsed I-V characteristics of an $L_g = 1.2 \mu\text{m}$ device for $8 \text{ ns} \leq T_d \leq 10 \mu\text{s}$ are shown in Fig. 4 for a wide range of V_{DS} and V_{GS} . Two observations can be made: *i*) there is no kink for short T_d (below 10 ns); *ii*) the kink turns on first and rises faster the higher V_{DS} is. Similar results are obtained for $L_g = 2 \mu\text{m}$ devices. These observations are consistent with reports in the literature on output conductance measurements of both InAlAs/InGaAs/InP HEMTs [3] and InAlAs/InGaAs/InAlAs MESFETs [14] in which no kink is observed at high frequencies despite its prominence at DC.

To further analyze our results, we have defined a “kink” current as follows:

$$\Delta I_D(T_d) = I_D(T_d) - [I_{D,prek}(T_d) + g_d(V_{DS} - V_{DS,prek})] \quad (1)$$

where $I_{D,prek}$, $V_{DS,prek}$, and g_d are respectively the “pre-kink” drain current, drain-to-source voltage,

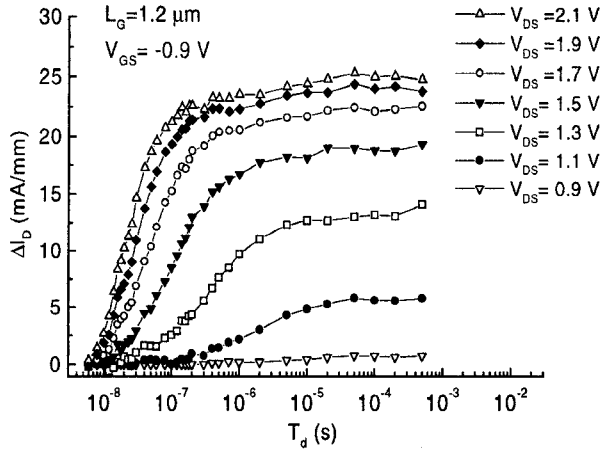


Figure 5: ΔI_D as a function of T_d for different values of V_{DS} but constant V_{GS} .

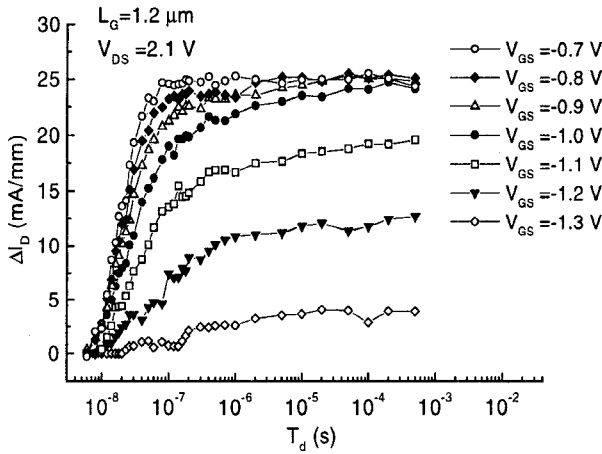


Figure 6: ΔI_D as a function of T_d for different values of V_{GS} but constant V_{DS} .

and saturation output conductance, and $V_{DS,sat} \leq V_{DS,prek} \leq V_{DS}$. In other words, ΔI_D is the drain current exceeding the “pre-kink” saturation drain current after output conductance compensation. Note that, as seen in fig. 4, $I_{D,prek}$ is slightly time dependent. The origin of this is not known. Eq. 1 accounts for this effect.

We plot in fig. 5 ΔI_D as a function of T_d for different values of V_{DS} ($V_{GS} = -0.9$ V). Some peculiar features of the kink can be observed: ΔI_D increases with V_{DS} but seems to saturate for sufficient large values of V_{DS} . This is the standard DC behavior of the kink [8, 12]. Dynamically, the rate at which ΔI_D builds up with time is faster the higher V_{DS} is. Interestingly, the kink’s saturation also gets sharper for increasing V_{DS} .

Let us now examine the characteristics of the kink dynamics for different values of V_{GS} and constant V_{DS} ($V_{DS} = 2.1$ V). The following features can be observed: *i*) the DC magnitude of ΔI_D increases

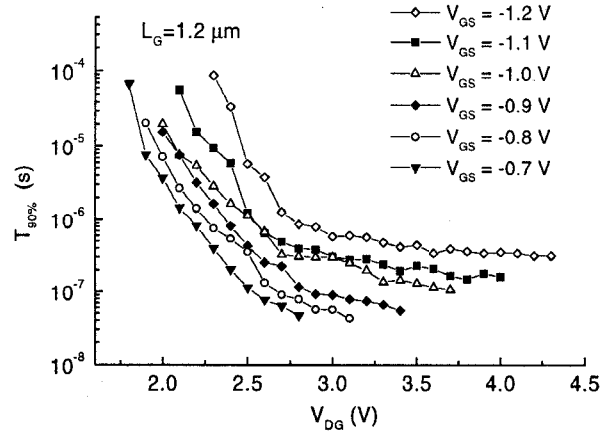


Figure 7: $T_{90\%}$, the time it takes for the kink to reach 90% of its final DC value, as a function of V_{DG} for different values of V_{GS} .

as V_{GS} increases above threshold. *ii*) For -0.9 V $\leq V_{GS} \leq -0.7$ V, the DC magnitude of ΔI_D is about the same. *iii*) The kink saturates faster the higher V_{GS} is.

The above results show that the kink’s characteristic time constant is strongly dependent on both V_{DS} and V_{GS} . This can be seen in a more quantitative way by examining the rise time of the kink, $T_{90\%}$, which we define as the time for ΔI_D to rise to 90% of its final DC value. $T_{90\%}$ is plotted in fig. 7 as a function of V_{DG} for different values of V_{GS} . $T_{90\%}$ is found to be a strong function of V_{GS} and V_{DG} for $V_{DG} \leq 2.8$ V. For $V_{GS} = -0.7$ V, for example, $T_{90\%}$ drops by three decades, from ~ 100 μ s down to ~ 50 ns, as V_{DG} increases from 1.7 to 2.8 V. Interestingly, $T_{90\%}$ becomes rather independent of V_{DG} for $V_{DG} \geq 2.8$ V. Note also that $T_{90\%}$ is smaller for constant V_{DG} but increasing values of V_{GS} . Clearly, the dynamics of the kink are not characterized by a single time constant that is independent of V_{DS} and V_{GS} .

The data presented in this work should be instrumental in formulating a hypothesis for the physical origin of the kink effect in InAlAs/InGaAs HEMTs.

IV. Conclusions

In summary, we have carried out for the first time pulsed measurements of the kink dynamics of InAlAs/InGaAs on InP HEMTs in the nanosecond regime. Our measurements show that the kink’s characteristic time constant is characterized by two regimes: for small values of V_{DG} , it decreases exponentially with V_{DG} ; on the other hand, for large values of V_{DG} , it becomes independent of V_{DG} . Time constants between 50 ns and 100 μ s have been observed.

Acknowledgments

This research has been founded by JSEP (DAAH04-95-1-0038), JSEP Fellowship (F49620-96-1-0232), NSF-PYI (9157305-ECS), and Texas Instruments. The authors would like to thank J. Liu and A. Swanson from Lockheed-Martin for their support and advice.

References

- [1] A. S. Brown, U. K. Mishra, C. S. Chou, C. E. Hooper, M. A. Melendes, M. Thompson, L. E. Larson, S. E. Rosenbaum, and M. J. Delaney, "AlInGaAs-GaInAs HEMT's utilizing low-temperature AlInAs buffers grown by MBE," *IEEE Electron Device Lett.*, vol. 10, no. 12, pp. 565-568, 1989.
- [2] T. Zimmer, D. Ouro Bodi, J. M. Dumas, N. Labat, A. Touboul, and Y. Danto, "Kink effect in HEMT structures: A trap-related semi-quantitative model and an empirical approach for spice simulation," *Solid-State Electron.*, vol. 35, no. 10, pp. 1543-1548, 1992.
- [3] W. Kruppa and J. B. Boos, "Examination of the kink effect in InAlAs/InGaAs/InP HEMT's using sinusoidal and transient excitation," *IEEE Trans. Electron Devices*, vol. 42, no. 10, pp. 1717-1723, 1995.
- [4] K. Kunihiro, H. Yano, N. Goto, and Y. Ohno, "Numerical analysis of kink effect in HJFET with heterobuffer layer," *IEEE Trans. Electron Devices*, vol. 40, no. 3, pp. 493-497, 1993.
- [5] G. G. Zhou, A. F. Fischer-Colbrie, and J. S. Harris, "I-V kink in InAlAs/InGaAs MOD-FET's due to weak impact ionization in the InGaAs channel," in *6th Int. Conf. on InP and Rel. Mater.*, Mar. 1994, pp. 435-438.
- [6] T. Akazaki, H. Takayanagi, and T. Enoki, "Kink effect in an InAs-inserted-channel InAlAs/InGaAs inverted HEMT at low temperature," *IEEE Electron Device Lett.*, vol. 17, no. 7, pp. 378-380, 1996.
- [7] B. Brar and H. Kroemer, "Influence of impact ionization on the drain conductance of InAs/AlSb quantum well HFET's," *IEEE Electron Device Lett.*, vol. 16, no. 12, pp. 548-550, 1995.
- [8] M. H. Somerville, J. A. del Alamo, and W. Hoke, "Direct correlation between impact ionization and the kink effect in InAlAs/InGaAs HEMT's," *IEEE Electron Device Lett.*, vol. 17, no. 10, pp. 473-475, 1996.
- [9] M. Chertouk, H. Heiß, D. Xu, S. Kraus, W. Klein, G. Böhm, G. Tränkle, and G. Weimann, "Metamorphic InAlAs/InGaAs HEMT's on GaAs substrates with composite channels and f_{max} of 350 GHz," *7th Intl. Conf. on InP and Rel. Mat.*, pp. 737, 1995.
- [10] Y. Hori and M. Kuzuhara, "Improved model for the kink effect in AlGaAs/InGaAs heterojunction FET's," *IEEE Trans. Electron Devices*, vol. 41, no. 12, pp. 2262-2266, 1994.
- [11] T. Enoki, T. Kobayashi, and Y. Ishii, "Device technologies for InP-based HEMT's and their applications to IC's," *IEEE GaAs IC symp.*, 1994, pp. 337-339.
- [12] M. H. Somerville, J. A. del Alamo, and W. Hoke, "A new physical model for the kink effect on InAlAs/InGaAs HEMT's," in *1995 Int. Electron Devices Meeting Tech. Dig.*, pp. 201-204.
- [13] A. Platzker, A. Palevsky, S. Nash, W. Struble, and Y. Tajima, "Characterization of GaAs devices by a versatile pulsed I-V measurement system" *1990 IEEE MTT Symposium Digest*, pp. 1137-1140.
- [14] J. B. Kuang, P. J. Tasker, G. W. Wang, Y. K. Chen, L. F. Eastman, O. A. Aina, H. Hier, and A. Fathimulla, "Kink effect in submicrometer-gate MBE-grown InAlAs/InGaAs/InAlAs Heterojunction MESFET's," *IEEE Electron Device Lett.*, vol. 9, no. 12, pp. 630-632, 1988.